

# Vibrational Spectral Investigations and Bio-Markers of Bronchodilatic Drug 1,3-dimethylxanthine

Y. Sheeba Sherlin<sup>a,1</sup>, T.Vijayakumar<sup>b</sup>, S.D.D. Roy<sup>c</sup> and V.S. Jayakumar<sup>d,\*</sup>

<sup>a</sup>Research Scholar, Department of Physics and Research Centre, Nesamony Memorial Christian College, Marthandam-629165, Tamil Nadu, India affiliated to Manonmaniam Sundaranar University, Abishekapatti, Tirunelveli-627012, Tamil Nadu, India.

<sup>b</sup>Department of Physics and Nanotechnology, SRM University, Kattankulathur, Kancheepuram-603203, India.

<sup>c</sup>Department of Physics and Research Centre, Nesamony Memorial Christian College, Marthandam-629165, Tamil Nadu, India

<sup>d</sup>Mar Baselios Institute of Technology, Anchal- 691306, Kerala, India.

\*Corresponding author: [vsjkumar@gmail.com](mailto:vsjkumar@gmail.com)

## Abstract

The drug action of Bronchodilatic Drug 1,3-dimethylxanthine (THP) are mediated by the inhibition of phosphodiesterase (PDE) and increase of intracellular cyclic adenosine monophosphate (cAMP) which mediates smooth muscular mediations. The vibrational spectral investigations of THP and the bio-markers of methylxanthine bronchodilators along with DFT computations explains the structural and bonding features, charge-transfer interactions, nature of hydrogen bonding etc. The strong and simultaneous occurrence of 8a mode in IR and Raman spectra reveals the involvement of benzene ring in the intermolecular charge transfer interaction through N-H...O hydrogen bonding. The bathochromic shift of  $\pi \rightarrow \pi^*$  band by 25 nm is due to the planarity of xanthine ring and the consequent extensive conjugation of lone pair electrons present in the nitrogen atoms of the pyrimidine and imidazole rings that gives an additional absorption band at  $288 \text{ cm}^{-1}$ . The spectral bio-marker bands of methylxanthine based bronchodilatic drugs, corresponding to ring C=C stretching *ca*  $1599 \text{ cm}^{-1}$  (8a mode) and C=O stretching vibrations *ca*  $1650 \text{ cm}^{-1}$  stretching vibrations are found to be strongly and simultaneously active in both IR and Raman spectra as observed in other bronchodilators *viz*, caffeine and theobromine. It is observed that the THP molecule possesses reasonably high dipole moment results in moderate  $\beta_{\text{total}}$  value which favours charge transfer interactions that help in binding with the receptor phosphodiesterase enzyme. THP in the binding pocket is stabilized through the attractive non-covalent T-shaped  $\pi$ - $\pi$  interaction,  $\pi$ -cation interactions and  $\pi$ -alkyl interactions between the aromatic rings of THP with the amino acid residues suggest that through these interactions the ligand THP binds with albumin protein that inhibits the synthesis of phosphodiesterase enzyme and other mediators in the process of improving its anti-asthmatic activity.

**Keywords:** FT-Raman; Bronchodilatic; Drug activity; DFT; Xanthine ring; Bio-Marker Bands

<sup>1</sup> Permanent Address: Department of Physics, Scott Christian College (Autonomous), Nagercoil-629003, Tamil Nadu, India.

## 1. Introduction

Bronchodilators are a type of medication that makes breathing easier by relaxing the muscles and increasing the airflow in the lungs [1]. Theophylline (THP) has been one of the most commonly used bronchodilator and respiratory simulator for the treatment of acute and chronic asthmatic conditions [2,3]. THP is mainly extracted from green tea leaves and is a long-acting bronchodilator available in oral and injectable form [4]. It is a promising central nervous system (CNS) stimulant and has been used in stimulation of respiration, augmentation of cardiac inotropy and chronotropy, relaxation of smooth muscle including bronchi and blood vessels other than cerebral and as diuretics [5]. THP belongs to methylxanthine derivative and xanthine is a purine based heterocyclic organic compounds coupled with pyrimidinedione and imidazole rings.

Vibrational spectroscopy has been shown to be an excellent analytical technique for the identification and determination of pharmaceuticals and biochemical [6-8]. The present work deals with the vibrational spectral investigations of THP and the bio-markers of methylxanthine bronchodilators along with DFT computations to explore the structural and bonding features, charge-transfer interactions, chemical activity descriptors, molecular docking, cytotoxicity, nature of hydrogen bonding etc.

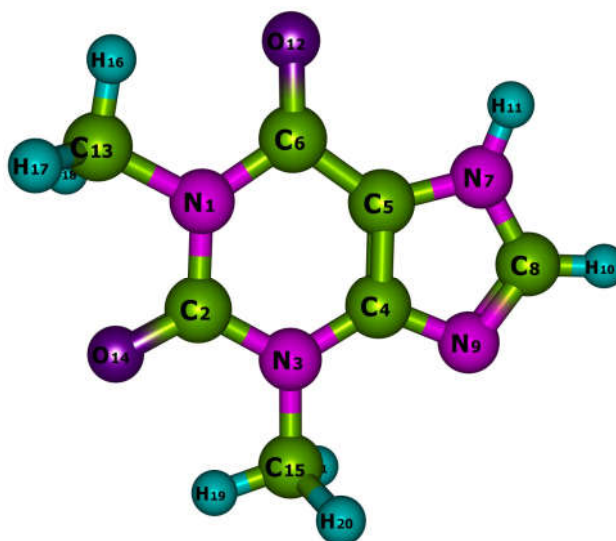


Fig.1 Optimized molecular structure of THP

## 2 Materials and Methods

### 2.1 Experimental

The bronchodilatic drug THP (1,3-dimethylxanthine) (Fig.1), procured from Aldrich (99.9 %) was used without further purification. The BRUKER RFS 27: FT-Raman spectrometer with an Nd:YAG laser at 1064 nm as the excitation source having resolution of  $2\text{ cm}^{-1}$  was used to measure the NIR-FT Raman spectrum in the region  $4000\text{-}50\text{ cm}^{-1}$ . The FTIR spectrum was recorded using Perkin-Elmer GX FT-IR spectrometer with the sample in KBr matrix having a resolution of  $4\text{ cm}^{-1}$  in the region  $4000\text{-}400\text{ cm}^{-1}$ .

## 2.2 Computational Details

The structural optimization of THP was performed with Gaussian 09W program package [9] using DFT method with B3LYP/6-311++G(d,p) basis set. The computed harmonic vibrational wavenumbers were uniformly scaled down by 0.9679 to account for systematic errors owing to harmonic approximation [10]. The vibrational modes are assigned on the basis of potential energy distribution (PED) analysis using VEDA 4 program [11,12].

## 3. Results and Discussion

### 3.1 Structural Properties

The X-ray diffraction (XRD) data of THP has been reported [13]. The optimized structural parameters of THP at B3LYP/6-311++G(d,p) basis set and the respective values from X-ray diffraction data are listed in Table 1. In THP, all dihedral angles in the benzene and imidazole ring not differ significantly from the mean observed value that shows both rings do not deviate significantly from planarity. The bond lengths of C<sub>6</sub>=O<sub>12</sub> and C<sub>2</sub>=O<sub>14</sub> bonds are measured to be 1.239 and 1.22 Å which is higher than the standard C=O bond length. It is observed that the C<sub>6</sub>=O<sub>12</sub> bond is elongated considerably due to the formation of intermolecular N-H...O hydrogen bonding and C<sub>2</sub>=O<sub>14</sub> is involved in C-H...O intermolecular hydrogen bonding. The C<sub>4</sub>=C<sub>5</sub> bond length connecting two rings is found to be 1.37 Å which is slightly lower than the aromatic C=C bonds that plays a vital role in the delocalization of the fused xanthine ring in THP.

The bond length N<sub>7</sub>-H<sub>11</sub> is measured to be 0.98 Å while the computed bond length is found to be 1.01 Å. The experimental N<sub>7</sub>-H<sub>11</sub> bond length is shorter than the predicted bond length which is due to intermolecular N-H...O hydrogen bond resulting in the formation of dimer between two crystallographically different molecules. The measured C-H bond lengths of methyl 1 (1-position of methylxanthine) group are found shorter than the other C-H bond lengths by 0.04 Å showing the involvement of methyl C-H bond in the formation of intermolecular C-H...O hydrogen bonding.

**Table 1** Experimental and Optimized geometric parameters of THP at B3LYP/6-311++G(d,p)

Bond Length	Exp <sup>a</sup> (Å)	Theo (Å)	Bond angle	Exp <sup>a</sup> (°)	Theo (°)	Dihedral angle	Exp <sup>a</sup> (°)	Theo (°)
N <sub>1</sub> -C <sub>2</sub>	1.38	1.41	C <sub>2</sub> -N <sub>1</sub> -C <sub>6</sub>	126.3	126.946	C <sub>3</sub> -C <sub>2</sub> -N <sub>1</sub> -C <sub>6</sub>	1.08	-0.0024
N <sub>1</sub> -C <sub>6</sub>	1.38	1.42	C <sub>2</sub> -N <sub>1</sub> -C <sub>13</sub>	115	115.147	O <sub>14</sub> -C <sub>2</sub> -N <sub>1</sub> -C <sub>6</sub>	178.84	180
N <sub>1</sub> -C <sub>13</sub>	1.46	1.47	C <sub>6</sub> -N <sub>1</sub> -C <sub>13</sub>	118.7	117.905	C <sub>3</sub> -C <sub>2</sub> -N <sub>1</sub> -C <sub>13</sub>	179.14	179.99
C <sub>2</sub> -N <sub>3</sub>	1.41	1.39	N <sub>1</sub> -C <sub>2</sub> -N <sub>3</sub>	117	116.967	O <sub>14</sub> -C <sub>2</sub> -N <sub>1</sub> -C <sub>13</sub>	0.96	0.001
C <sub>2</sub> -O <sub>14</sub>	1.22	1.22	N <sub>1</sub> -C <sub>2</sub> -O <sub>14</sub>	121.2	120.755	C <sub>2</sub> -N <sub>1</sub> -C <sub>6</sub> -C <sub>5</sub>	-1.63	0.0019
N <sub>3</sub> -C <sub>4</sub>	1.37	1.37	N <sub>3</sub> -C <sub>2</sub> -O <sub>14</sub>	121.8	122.277	C <sub>2</sub> -N <sub>1</sub> -C <sub>6</sub> -O <sub>12</sub>	178.83	-180
N <sub>3</sub> -C <sub>15</sub>	1.47	1.46	C <sub>2</sub> -N <sub>3</sub> -C <sub>4</sub>	119.3	119.501	C <sub>13</sub> -N <sub>1</sub> -C <sub>6</sub> -C <sub>5</sub>	178.58	-180
C <sub>4</sub> -C <sub>5</sub>	1.37	1.38	C <sub>2</sub> -N <sub>3</sub> -C <sub>15</sub>	118.3	120.045	C <sub>13</sub> -N <sub>1</sub> -C <sub>6</sub> -O <sub>12</sub>	-0.96	-0.0012
C <sub>4</sub> -N <sub>9</sub>	1.36	1.36	C <sub>4</sub> -N <sub>3</sub> -C <sub>15</sub>	122.4	120.454	C <sub>2</sub> -N <sub>1</sub> -C <sub>13</sub> -H <sub>16</sub>	-127.6	-180

C <sub>5</sub> -C <sub>6</sub>	1.42	1.43	N <sub>3</sub> -C <sub>4</sub> -C <sub>5</sub>	122.1	121.705	C <sub>2</sub> -N <sub>1</sub> - C <sub>13</sub> -H <sub>17</sub>	115.36	59.704
C <sub>5</sub> -N <sub>7</sub>	1.39	1.38	N <sub>3</sub> -C <sub>4</sub> -N <sub>9</sub>	125.9	126.633	C <sub>2</sub> -N <sub>1</sub> - C <sub>13</sub> -H <sub>18</sub>	-2.11	-59.7
C <sub>6</sub> -O <sub>12</sub>	1.24	1.22	C <sub>5</sub> - C <sub>4</sub> -N <sub>9</sub>	111.3	111.662	C <sub>6</sub> -N <sub>1</sub> -C <sub>13</sub> -H <sub>16</sub>	-21.88	0.0024
N <sub>7</sub> -C <sub>8</sub>	1.34	1.36	C <sub>4</sub> -C <sub>5</sub> -C <sub>6</sub>	122.9	123.917	C <sub>6</sub> -N <sub>1</sub> - C <sub>13</sub> -H <sub>17</sub>	-131.4	-120.3
N <sub>7</sub> -H <sub>11</sub>	0.98	1.01	C <sub>4</sub> -C <sub>5</sub> -N <sub>7</sub>	105.3	104.868	C <sub>6</sub> -N <sub>1</sub> - C <sub>13</sub> -H <sub>18</sub>	177.7	120.3
C <sub>8</sub> -N <sub>9</sub>	1.34	1.33	C <sub>6</sub> -C <sub>5</sub> -N <sub>7</sub>	131.8	131.216	N <sub>1</sub> -C <sub>2</sub> -N <sub>3</sub> - C <sub>4</sub>	-1.63	0.001
C <sub>8</sub> -H <sub>10</sub>	1	1.08	N <sub>1</sub> - C <sub>6</sub> -C <sub>5</sub>	112.3	110.963	N <sub>1</sub> -C <sub>2</sub> -N <sub>3</sub> -C <sub>15</sub>	52.27	180
C <sub>13</sub> -H <sub>16</sub>	0.97	1.09	N <sub>1</sub> - C <sub>6</sub> -O <sub>12</sub>	120.6	123.009	O <sub>14</sub> -C <sub>2</sub> -N <sub>3</sub> - C <sub>4</sub>	179.97	-180

<sup>a</sup>Taken from Ref [13]

### 3.2 Vibrational Analysis of Bronchodilator Drug THP

The vibrational spectral analysis of THP has been performed on the basis of the characteristic vibrations of Pyrimidine ring, Imidazole ring Methyl, Carbonyl, C-H and N-H groups. The computed wavenumbers are compared with the experimental FT-IR and FT-Raman wavenumbers and their assignments are given in Table 2. The experimental and calculated Raman and IR spectra of THP are shown in Fig. 2 and 3.

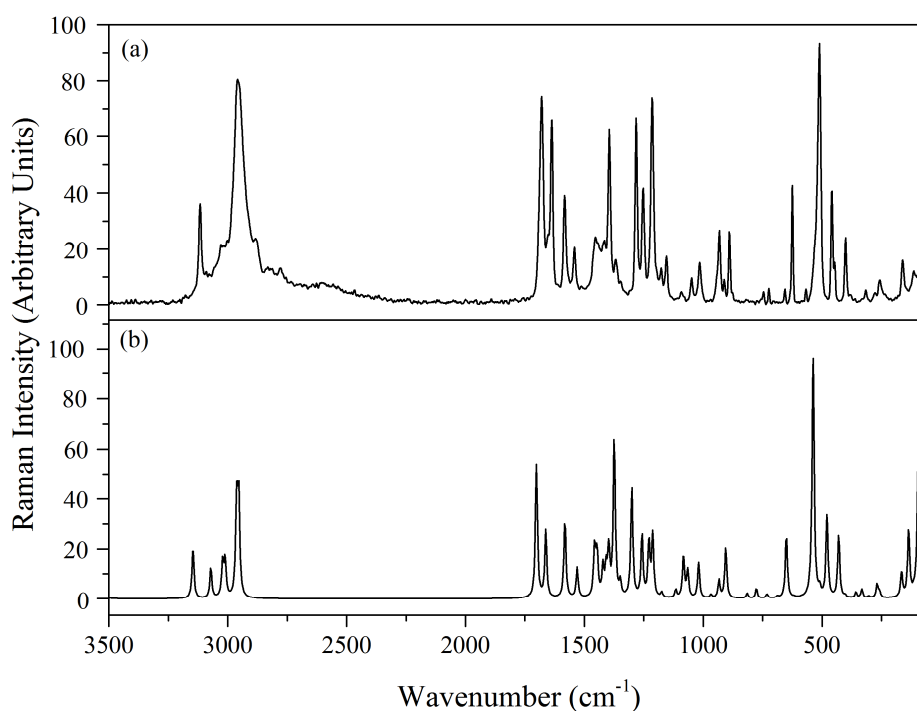


**Fig. 2** Combined experimental (a) and theoretical (b) Raman spectrum of THP

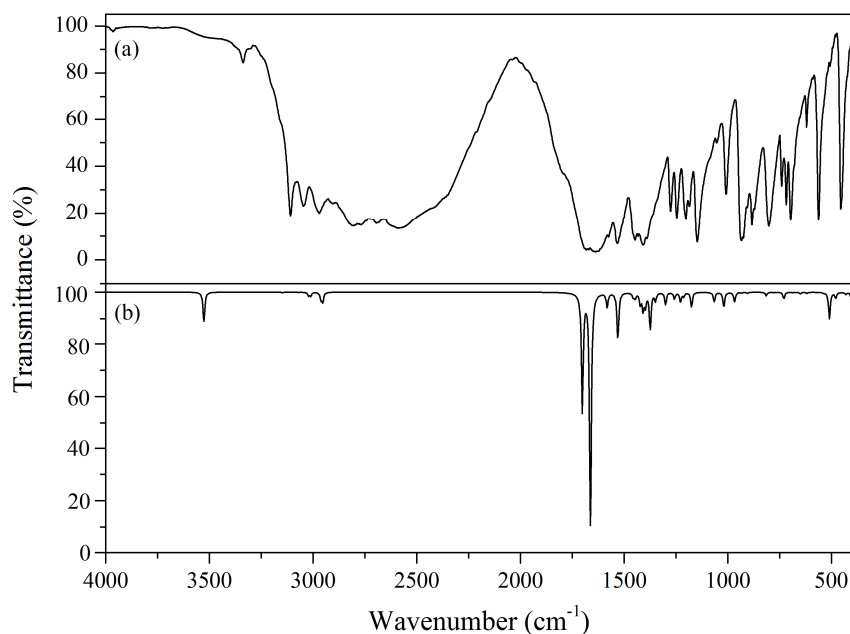


**Fig. 3** Combined experimental (a) and theoretical (b) IR spectrum of THP

### 3.2.1 Xanthine Ring Vibrations

#### *Pyrimidine Ring Vibrations*

Most of the substituted pyrimidine exhibit four bands in the range  $1600\text{-}1375\text{ cm}^{-1}$  due to aromatic ring stretches [14]. In THP, the vibration of 8a mode appears as very strong bands in IR at  $1608\text{ cm}^{-1}$  and at  $1610\text{ cm}^{-1}$  in Raman. A very strong band at  $1566\text{ cm}^{-1}$  in IR and weak band at  $1569\text{ cm}^{-1}$  in Raman corresponds to 8b mode.

The fused ring aromatic such as benzene ring fused to five or six membered ring heterocyclics have ring stretch bands in the region  $1600\text{-}1500\text{ cm}^{-1}$  [15]. In THP six membered pyrimidine ring is fused with a five membered Imidazole ring so that they give rise to a fused ring stretch at strong band at  $1608\text{ cm}^{-1}$  in IR. The strong and simultaneous occurrence of 8a mode in IR and Raman spectra explains the involvement of benzene ring in the intermolecular charge transfer interaction through  $\text{N-H}\cdots\text{O}$  hydrogen bonding.

#### *Imidazole Ring Vibrations*

In general, azoles have three or four band in the region  $1670\text{-}1320\text{ cm}^{-1}$  due to  $\text{C}=\text{C}$  and  $\text{C}=\text{N}$  stretching vibrations [16]. The most characteristic vibrations of the heterocyclic imidazole ring is the stretching mode of  $\text{C}_4=\text{C}_5$  bond. In THP, this mode is observed at  $1608$  and  $1313\text{ cm}^{-1}$  in IR as very strong band and its counterpart appears strong in Raman at  $1610$  and  $1314\text{ cm}^{-1}$  which is obviously in the range of protonated imidazole. The imidazole ring breathing mode is identified at  $926\text{ cm}^{-1}$  in IR and at  $927\text{ cm}^{-1}$  in Raman as intense bands. The imidazole ring deformation modes appear as intense IR band at  $1049$  and at  $1051\text{ cm}^{-1}$  in Raman. In solid phase, five membered heteroatomic compounds with two or more nitrogen atoms in the ring have a broad absorption at  $2800\text{-}2600\text{ cm}^{-1}$

due to the N-H...O bond [48]. In THP, this mode appears as a strong broad band at 2713 and 2607  $\text{cm}^{-1}$  due to intermolecular N-H...O hydrogen bonding.

**Table 2** Calculated vibrational wavenumbers, measured infrared and Raman band positions and their assignments of THP at B3LYP/6-311++G(d,p) level.

$\nu_{\text{scaled}}$	$\nu_{\text{IR}}$	$\nu_{\text{Raman}}$	PED (%)
3529	3346w		$\nu_{\text{N}_7-\text{H}_{11}}$ (99)
3148	3121vs	3121m	$\nu_{\text{C}_8-\text{H}_{10}}$ (99)
3073	3060vs		$\nu_{\text{C}_{15}-\text{H}_{19}}$ (86)
3023	2984s		$\nu_{\text{C}_{13}-\text{H}_{17}}$ (50)+ $\nu_{\text{C}_{13}-\text{H}_{18}}$ (50),
2964		2966s	$\nu_{\text{C}_{15}-\text{H}_{20}}$ (50)+ $\nu_{\text{C}_{15}-\text{H}_{21}}$ (44)
2955	2822vs		$\nu_{\text{C}_{13}-\text{H}_{17}}$ (41)+ $\nu_{\text{C}_{13}-\text{H}_{18}}$ (42)+ $\nu_{\text{C}_{13}-\text{H}_{16}}$ (16)
	2713 s 2607 vs		N-H...O stretch
1703	1715vs 1702 vs	1706 s	$\nu_{\text{C}_2-\text{O}_{14}}$ (38)+ $\text{C}_6-\text{O}_{12}$ (34)
1663	1669 vs	1664s	$\nu_{\text{C}_6-\text{O}_{12}}$ (29)+ $\nu_{\text{C}_2-\text{O}_{14}}$ (17)
1583	1608vs	1610s	$\nu_{\text{C}_4-\text{C}_5}$ (41)+ $\nu_{\text{N}_3-\text{C}_4}$ (24)
1531	1566vs	1569w	$\beta_{\text{C}_5-\text{C}_6-\text{N}_7}$ (35)
1449	1483vs		$\beta_{\text{H}_{19}-\text{C}_{15}-\text{H}_{21}}$ (77)+ $\tau_{\text{C}_{15}-\text{H}_{19}-\text{N}_3-\text{H}_{20}}$ (13)
1446	1468vs		$\beta_{\text{H}_{16}-\text{C}_{13}-\text{H}_{18}}$ (76)+ $\tau_{\text{C}_{13}-\text{H}_{16}-\text{N}_1-\text{H}_{17}}$ (13)
1423	1444vs		$\nu_{\text{C}_9-\text{C}_8}$ (32)+ $\beta_{\text{H}_{10}-\text{C}_8-\text{N}_9}$ (12)+ $\nu_{\text{N}_7-\text{C}_8}$ (10)
1409	1426vs	1425s	$\tau_{\text{C}_{13}-\text{H}_{17}-\text{H}_{18}-\text{H}_{16}}$ (30)+ $\tau_{\text{C}_{15}-\text{H}_{20}-\text{H}_{21}-\text{H}_{19}}$ (26)
1374	1313s	1314s	$\beta_{\text{H}_{11}-\text{N}_7-\text{C}_5}$ (20)+ $\tau_{\text{C}_{13}-\text{H}_{17}-\text{H}_{18}-\text{H}_{16}}$ (12), $\nu_{\text{N}_7-\text{C}_8}$ (11)
1349	1284s	1285 m	$\nu_{\text{N}_3-\text{C}_4}$ (19)+ $\nu_{\text{N}_7-\text{C}_8}$ (13)+ $\nu_{\text{C}_4-\text{C}_5}$ (11)
1301	1241s	1247s	$\nu_{\text{C}_9-\text{C}_8}$ (20)+ $\beta_{\text{C}_5-\text{N}_7-\text{C}_8}$ (13)+ $\tau_{\text{C}_2-\text{N}_3-\text{C}_4-\text{N}_9}$ (12)
1175	1187 vs	1188 w	$\text{N}_7-\text{C}_8$ (24)+ $\beta_{\text{H}_{10}-\text{C}_8-\text{N}_9}$ (14)+ $\beta_{\text{H}_{20}-\text{C}_{15}-\text{N}_3}$ (12)+ $\tau_{\text{C}_{15}-\text{H}_{19}-\text{N}_3-\text{H}_{20}}$ (10)
968	977 vs		$\beta_{\text{C}_5-\text{N}_7-\text{C}_8}$ (13)
934	968vs	969 m	$\nu_{\text{N}_3-\text{C}_{15}}$ (14)+ $\beta_{\text{C}_5-\text{N}_7-\text{C}_8}$ (13)+ $\beta_{\text{C}_4-\text{N}_9-\text{C}_8}$ (13)
905	926 s	927 m	$\beta_{\text{C}_4-\text{N}_9-\text{C}_8}$ (36)+ $\text{N}_3-\text{C}_{15}$ (12)
815	846 s		$\tau_{\text{H}_{10}-\text{C}_8-\text{N}_9-\text{C}_4}$ (85)

\*Wilson numbering scheme has been used for ring modes,  $\nu$ -stretching,  $\beta$ -bending,  $\tau$ -torsion, asym-asymmetric, symmetric, vvs-very very strong, vs-very strong, s-strong, m-medium, w-weak, vw-very weak

### *Methylated Xanthine Ring Vibrations*

Methylxanthines are methylated derivative of xanthine commonly used for their effects as mild stimulants on various organ systems such as central nervous system (CNS), cardiovascular and skeletal muscles. It is a heterocyclic organic compound coupled with pyrimidinedione and imidazole rings and THP belongs to this derivative. The xanthine ring C=C/C-N stretching modes [17] are observed at 1608 and 1566  $\text{cm}^{-1}$  in IR and at 1610 and 1569  $\text{cm}^{-1}$  in Raman as most intense bands. The xanthine ring stretching mode is identified at 1248  $\text{cm}^{-1}$  as intense IR band and at 1285  $\text{cm}^{-1}$  in Raman which has the contribution of pyrimidine ring, imidazole ring along with the bridging C=C stretching vibrations being calculated at 1349  $\text{cm}^{-1}$  [18]. The strong IR band at 968  $\text{cm}^{-1}$  and the Raman band at 969  $\text{cm}^{-1}$  can be attributed to the xanthine ring breathing vibration while trigonal xanthine ring mode is found at 610  $\text{cm}^{-1}$  as strong IR band.

### **3.2.2 Carbonyl Vibrations**

The C=O stretching vibration is expected to occur in the region 1715-1680  $\text{cm}^{-1}$  [19]. In xanthine, C=O attached to the pyrimidine ring gives rise to two strong bands and these modes appear in THP at 1715 and 1702  $\text{cm}^{-1}$  as most intense split IR bands and at 1706  $\text{cm}^{-1}$  as intense band in Raman, and another band occurs at 1669 and 1664  $\text{cm}^{-1}$  in IR and Raman, respectively, as strong bands. The former band is due to the carbonyl group C<sub>2</sub>=O<sub>14</sub> whose bond length is 1.22 Å which is involved in C-H...O intermolecular hydrogen bonding with imidazole C-H and methyl groups of neighbouring THP molecules. Likewise, the latter band is due to the carbonyl group C<sub>6</sub>=O<sub>12</sub> whose bond length is 1.239 Å, elongated by 0.019 Å, making intermolecular N-H...O hydrogen bonding with amine group of imidazole ring of adjacent THP molecules. The conjugation and influence of intermolecular hydrogen bonding network in the crystal results in the lowering of the stretching wavenumbers. The band associated with C=O stretching mode are found to be strongly and simultaneously active in both IR and Raman spectra. The greater electronegativity of these carbonyl oxygen atoms as compared to nitrogen helps in participating the binding reaction of THP molecules through hydrogen bond interaction with the protonated group of plasma protein.

### **3.2.3 Amine vibrations**

The ring N-H stretching mode of imidazole ring is correlated to the band observed at 3346  $\text{cm}^{-1}$  in IR. The observed N-H stretching wavenumber is found to be lower than the calculated wavenumber by 180  $\text{cm}^{-1}$  which is due to the formation of strong intermolecular N-H...O hydrogen bonding between N-H group attached to the imidazole ring and C=O group attached to the pyrimidine ring which is also substantiated by XRD [13]. The occurrence of additional strong IR bands at 2713 and 2607  $\text{cm}^{-1}$  indicates the existence strong N-H...O intermolecular hydrogen bonding. The N-H deformation mode is identified as intense band at 1313  $\text{cm}^{-1}$  in IR and 1314  $\text{cm}^{-1}$  in Raman, and this mode occurs strongly and simultaneously in IR and Raman spectra overlapping with imidazole ring stretching vibrations which clearly explain intermolecular charge transfer through N-H...O hydrogen bonding making lipophilicity to the drug molecule substantially contributes towards the binding of THP especially to the plasma proteins.

### 3.2.4 Methyl/Methine Vibrations

Methyl groups are generally referred to as electron donating substituent in the aromatic ring system. The asymmetric C-H stretching mode of CH<sub>3</sub> is expected in the region nearly 2980 cm<sup>-1</sup> and the symmetric counterpart around the region 2870 cm<sup>-1</sup> [20,21]. In THP, two methyl groups are attached to the pyrimidine ring, one is in the proximity (Methyl I) and another is not in the proximity (methyl II) of imidazole ring. The CH<sub>3</sub> I asymmetric stretching mode is identified at 3060 cm<sup>-1</sup> as very strong IR band and strong IR band at 2984 cm<sup>-1</sup> is attributed to CH<sub>3</sub> II asymmetric stretching vibrations. The symmetric stretching modes of CH<sub>3</sub> I and II manifest a medium Raman band at 2966 and at 2822 cm<sup>-1</sup> in IR, respectively. The changes in intensity of CH<sub>3</sub> stretching mode in IR and shift to higher wavenumbers are due to the influence of electronic effects resulting from hyperconjugation and induction of methyl group causing changes in intensity clearly indicate that methyl hydrogens are directly involve in the donation of electronic charge. Further, shifting of the stretching frequencies towards higher wavenumbers, intensity variation and methyl C-H bonds contraction (~0.961 Å) indicate the existence of C-H...O intermolecular 'improper or blue shifting' hydrogen bonding.

Generally, C-H stretching vibration of heterocyclic compounds gives rise to band in the region 3100-3000 cm<sup>-1</sup> and the C-H bond attached to the imidazole ring shows high frequency shift in C-H stretch which result from substituent changes. In THP, the imidazole ring C-H stretching mode is observed at 3121 cm<sup>-1</sup> in IR and Raman as intense bands, and the shifting of C-H stretching wavenumber towards higher wavenumber further substantiates the existence of intermolecular C-H...O 'blue-shifting' hydrogen bonding [20].

### 3.3 Spectral Bio-Marker Bands of Bronchodilatic Drugs

Structure-Activity relationship (SAR) is the qualitative correlation of chemical structure with a well-defined biological activity. Theophylline belongs to methylxanthine derivative and it has been used for the treatment of asthma and chronic obstructive pulmonary disease (COPD). The actions of theophylline are mediated by the inhibition of phosphodiesterase (PDE) and increase of intracellular cyclic adenosine monophosphate (cAMP) which mediates smooth muscular mediations. THP has more lipophilic characteristics [22] and therefore it can easily diffuse through cell membranes and cross the blood-brain barrier. The polarity of molecules and negative charges play a vital role for the interaction of THP with the plasma proteins through vander Waal's forces and electrostatic interaction. THP attributes to ionization through the removal of proton from N7 and becomes negatively charged, and the greater electronegativity of oxygen as compared to nitrogen suggests that the negative charge probably resides on the pyrimidinedione oxygen nucleus and this might be responsible for the binding of methylxanthine with plasma protein. The pyrimidinedione oxygen participates directly in the binding reaction, perhaps through hydrogen bond formation with a protonated grouping on the plasma protein. The strength of such a bond would be substantially increased if the oxygen were to possess a negative charge. In addition, it may be noted that a methyl substituent on the N1 position will increase the electron density around the oxygen through an inductive effect. The vibrational modes corresponding to these functional groups are responsible for the bronchodilatic activity (anti-asthmatic) and these bands are considered as the spectral bio-marker bands [23] for the identification of

methylxanthine based bronchodilatic drugs. The spectral bio-marker bands of methylxanthine based bronchodilatic drugs, corresponding to ring C=C stretching  $ca$   $1599\text{ cm}^{-1}$  (8a mode) and C=O stretching vibrations  $ca$   $1650\text{ cm}^{-1}$  stretching vibrations are found to be strongly and simultaneously active in both IR and Raman spectra as observed in other bronchodilators *viz.*, caffeine and theobromine [4].

### 3.4 Electronic properties

Electronic transitions provide the information about the presence of conjugated  $\pi$ -systems, and the existence of double and triple bonds. In THP, an absorption band at 263 nm (Fig. 4) is due to the presence of  $\alpha$ ,  $\beta$ -unsaturated aromatic carbonyl chromophores corresponding to  $\pi \rightarrow \pi^*$  transition. The bathochromic shift of  $\pi \rightarrow \pi^*$  band by 25 nm is due to the planarity of xanthine ring and the consequent extensive conjugation of lone pair electrons present in the nitrogen atoms of the pyrimidine and imidazole rings that gives an additional absorption band at  $288\text{ cm}^{-1}$  [24].

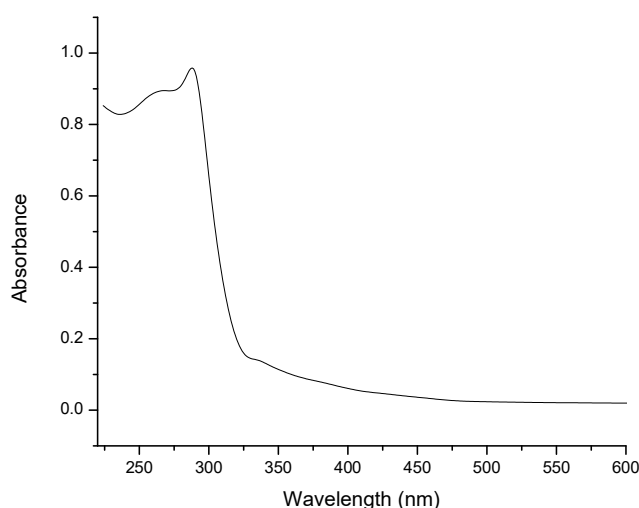


Fig. 4 UV-Visible absorption spectrum of THP

Time-dependent DFT calculations are performed at B3LYP/6-31G (d,p) method to study the nature of electronic transitions in terms of their oscillator strengths and energies. The scaled computed lowest-energy transition of THP observed at 280nm (4.438eV) and 275 nm (4.495 eV) with an oscillator strength of 0.0686 and 0.0472 can be correlated to  $n \rightarrow \pi^*$  and  $\pi \rightarrow \pi^*$  in gas phase.

### 3.5 Natural Bonding Orbital Analysis

The natural bond orbital (NBO) analysis was performed using NBO 3.1 program at B3LYP/6-311++G(d,p) level for THP monomer and dimer (Fig. 5). Second order perturbation theory analysis of Fock matrix in NBO basis is tabulated in Table 3. Hyperconjugative interactions of lone pair of oxygen  $n_2(\text{O}_{12})$  with vicinal antibonds  $\pi^*(\text{N}_{29}-\text{H}_{36})$  have energy contributions 4.66 kcal/mol, leading to N-H $\cdots$ O intermolecular hydrogen bonding interactions. The

strength of the C=O bond is higher than those of other bands which is confirmed by NBO occupancies of C<sub>6</sub>=O<sub>12</sub> and C<sub>2</sub>=O<sub>14</sub> bonds, larger than those of other bands. NBO analysis within rings reveals that C<sub>4</sub>-C<sub>5</sub>, and C<sub>8</sub>-C<sub>9</sub> bonds have two occupancies indicating that these bonds exhibit typical double bond characteristics. Stabilization energy E(2) associated with hyperconjugative interactions n<sub>2</sub>(O<sub>22</sub>) → σ\*(N<sub>7</sub>-H<sub>11</sub>) and n(2)O<sub>12</sub> → σ\*(N<sub>29</sub>-H<sub>36</sub>) are obtained as 7.15 and 7.21 kcal mol<sup>-1</sup> respectively which quantify the extend of intermolecular hydrogen bonding.

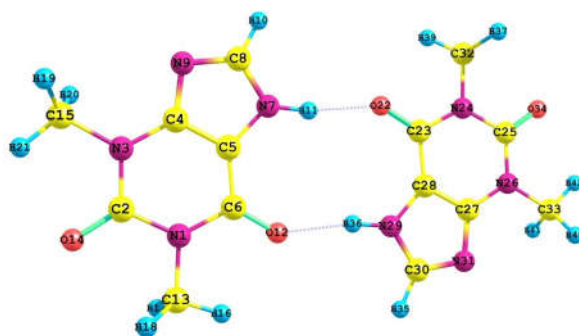


Fig. 5 Optimized Molecular Structure of THP Dimer

Table 3 Second order perturbation theory analysis of Fock matrix in NBO basis of THP

Donor (i)	ED(i) (e)	Acceptor (j)	ED (j) (e)	E(2) (kcal/ mol)	E(j)-E(i) (a.u)	F(i,j) (a.u)
π(C4 – C5)	1.967	σ*(C5 – N7)	0.020	1.37	1.09	0.035
σ(C4 – C5)	1.727	σ*(C8 – N9)	0.007	17.36	0.20	0.054
σ(C 8 - N9)	1.980	σ*(N 7 - H 11)	0.015	2.34	1.29	0.049
π(C8 - N9)	1.816	π*(C4 – C5)	0.434	28.74	0.33	0.094
n1(O12)	1.856	σ*(N 29 - H36)	0.038	7.21	1.13	0.081
n2(O12)	1.856	σ*(N 29 - H36)	0.038	5.66	0.72	0.058
n2(O12)	1.856	σ*(N1 - C6)	0.097	27.57	0.70	0.126
n2(O12)	1.856	σ*(C5 - C6)	0.056	16.47	0.69	0.097
n1(O22)	1.979	σ*(N 7 - H 11)	0.015	7.15	1.15	0.081

E(2)-Energy of hyperconjugative interactions (stabilization energy); E(j)-E(i)-Energy difference between donor i and acceptor j NBO orbitals; F(i,j)-Fock matrix element between i and j NBO orbitals; D-dimer; M-monomer

### 3.6 Molecular Electrostatic Potential (MESP) Analysis

The visual representation of chemically active sites in THP using MESP mapping is shown in Fig.8.9 and the generated ESP surfaces are represented by different colors. In THP, lone pair electrons providing stabilization to the molecule thereby enhance its hydrogen bonding. The title molecule is found to have more negative potential (red) around oxygen atoms attached to the pyrimidine ring and nitrogen atoms of xanthine ring responsible for

electrophilic activity while the positive potential (blue) is located over the hydrogen atoms attached to the imidazole ring responsible for nucleophilic reactivity with the receptor.

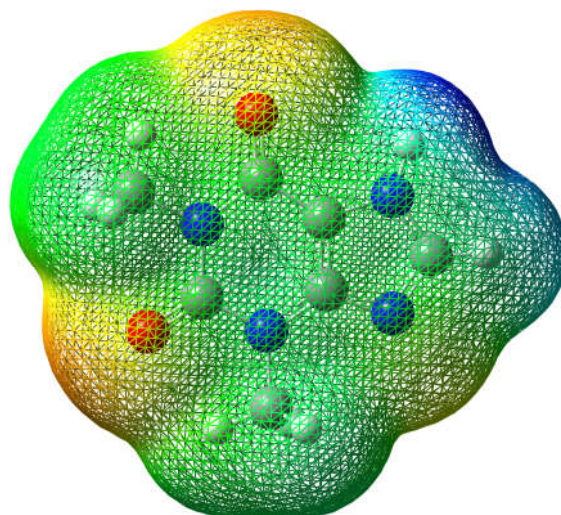


Fig. 6 Electrostatic potential mapping of THP

### 3.7 Frontier Molecular Orbital Analysis

The HOMO and LUMO plot for THP with the corresponding energies and energy gap are presented in Fig. 7. HOMO is localized over pyrimidine ring, imidazole ring, both carbonyl groups and a methyl group near to imidazole ring, and LUMO is located over pyrimidine ring, imidazole ring, both methyl groups and carbonyl group in the proximity of imidazole ring. Therefore, the charge density is transferred between methylated xanthine ring of THP molecules eventually explains charge transfer interactions take place from one molecule to another through N-H $\cdots$ O and C-H $\cdots$ O intermolecular hydrogen bonding. The calculated HOMO and LUMO energies are -0.238 eV and -0.0446 eV and the low energy gap (0.1934eV) results in high reactivity and low chemical stability.

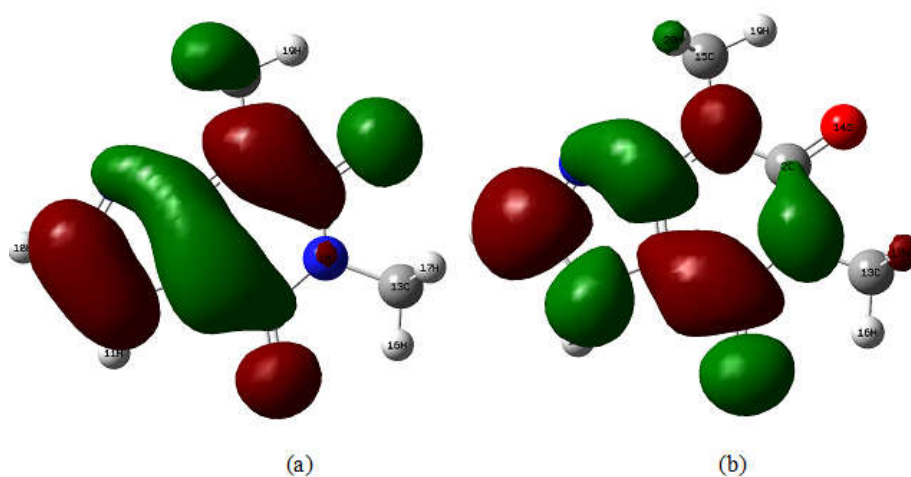


Fig. 7 (a) HOMO and (b) LUMO plot of THP

### 3.8 Dipole moment, polarizability and hyperpolarizability

The hyperpolarizabilities and polarizabilities characterize the response of a system with an electric field. When very-high-intensity electric fields are applied to a molecule, the induced polarization varies as a non-linear function of field strength. The first order hyperpolarizability ( $\beta$ ), polarizability ( $\langle\alpha\rangle$ ) and ground state dipole moment ( $\mu$ ) of THP are computed at B3LYP/6-311G(d,p) to be  $1.2066 \times 10^{-30}$  e.s.u (6 times that of urea),  $1.5586 \times 10^{-23}$  e.s.u and 1.393 Debye, respectively. It is observed that the THP molecule possesses reasonably high dipole moment results in reasonable high  $\beta_{\text{total}}$  value which favours charge transfer interactions that help in binding with the receptor phosphodiesterase enzyme.

### 3.9 Molecular Docking Analysis

Molecular docking study was performed with the aim to examine the binding mode of ligand with the receptor. THP was docked into the active site of albumin protein, 2VUE [25], obtained from Protein Data Bank to identify non-bonded and electrostatic interactions. Auto Dock binding energy for the protein 2VUE is -4.74 kcal/mol.

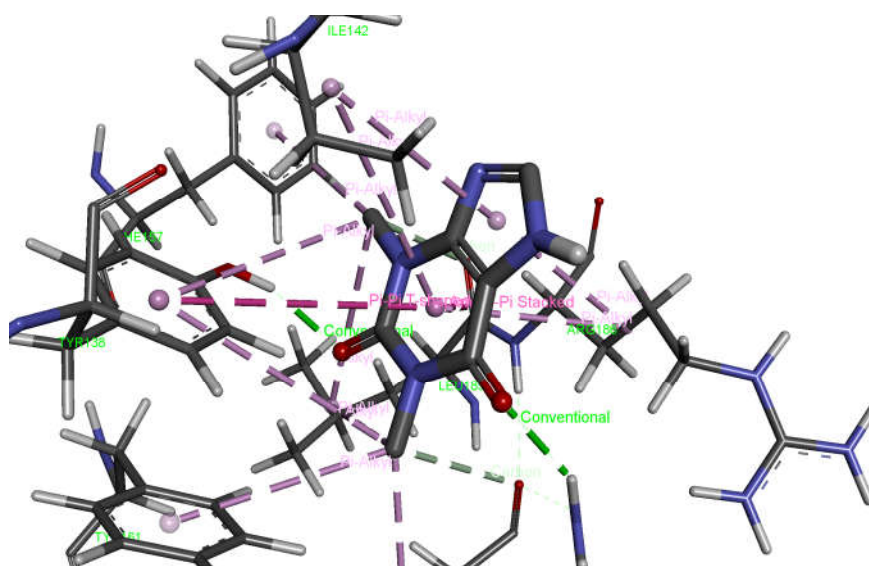


**Fig. 8** Docked conformation of THP in the binding site of 2VUE

It was observed that the molecule is preferred to interact with protein (Fig. 8) via intermolecular hydrogen bonding and non-bonded interactions. The carbonyl group attached to the pyrimidine ring near to the imidazole moiety bind with the amide group of arginine-117 residue through N-H $\cdots$ O intermolecular hydrogen bonding having H $\cdots$ O distances 2.21 Å. The another carbonyl group attached to the pyrimidine ring not in the proximity of imidazole ring also bind with carboxyl group of tyrosine-138 residue of the protein through O-H $\cdots$ O intermolecular hydrogen bonding and the corresponding H $\cdots$ O distances are 2.0 Å.

THP in the binding pocket is stabilized through the attractive non-covalent T-shaped  $\pi$ - $\pi$  interaction between the aromatic rings, from the pyrimidine moiety of THP with benzene ring of aromatic amino acid tyrosine-138 residue, binding distance equal to 5.40 Å. This is also evident by stacking interactions exist in the crystal structure of THP. T-shaped configured  $\pi$ - $\pi$  interaction is favorable due to the quadrupole interactions between the rings and it will increase their binding affinity. The THP ligand is also further stabilized by multiple  $\pi$ -cation interactions from the pyrimidine and imidazole ring with the various amino acids of 2VUE protein binding pocket. The geometric parameters of weak  $\pi$ - $\pi$  and  $\pi$ -alkyl interactions suggest that these interactions are of weak hydrogen bonds through which the ligand THP binds with serum albumin protein that inhibits the synthesis of phosphodiesterase enzyme and other mediators in the process of improving its anti-asthmatic activity.

#### 4. Conclusions

The detailed vibrational analysis of bronchodilatic drug 1,3-dimethylxanthine has been carried out using FT-IR and FT-Raman spectra aided by DFT calculations. It is inferred that the  $C_6=O_{12}$  bond is elongated considerably due to the formation of intermolecular N-H $\cdots$ O hydrogen bonding and  $C_2=O_{14}$  is involved in C-H $\cdots$ O intermolecular hydrogen bonding. The strong and simultaneous occurrence of 8a mode in IR and Raman spectra explains the involvement of benzene ring in the intermolecular charge transfer interaction through N-H $\cdots$ O hydrogen bonding. The xanthine ring C=C/C-N stretching modes are observed at 1608 and 1566  $cm^{-1}$  in IR and at 1610 and 1569  $cm^{-1}$  in Raman as most intense bands. The band associated with C=O stretching mode are found to be strongly and simultaneously active in both IR and Raman spectra. The observed N-H stretching wavenumber is found to be lower than the calculated wavenumber by 180  $cm^{-1}$  which is due to the formation of strong intermolecular N-H $\cdots$ O hydrogen bonding between N-H group attached to the imidazole ring and C=O group attached to the pyrimidine ring which is also substantiated by XRD. The N-H deformation mode occurs strongly and simultaneously in IR and Raman spectra overlapping with imidazole ring stretching vibrations which clearly explain intermolecular charge transfer through N-H $\cdots$ O hydrogen bonding making lipophilicity to the drug molecule substantially contributes towards the binding of THP especially to the plasma proteins. The vibrational modes corresponding to the pyrimidinedione oxygen and ring C=C moieties are responsible for the bronchodilatic activity (anti-asthmatic) and these bands are considered as the spectral bio-marker bands for the identification of methylxanthine based bronchodilatic drugs. The spectral bio-marker bands of methylxanthine based bronchodilatic drugs, corresponding to ring C=C stretching ca 1599  $cm^{-1}$  (8a mode) and C=O stretching vibrations ca 1650  $cm^{-1}$  stretching vibrations are found to be strongly and simultaneously active in both IR and Raman spectra as observed in other bronchodilators viz, caffeine and theobromine. It is observed that the THP molecule possesses reasonably high dipole moment results in reasonable high  $\beta_{total}$  value which favours charge transfer interactions that help in binding with the receptor phosphodiesterase enzyme. THP in the binding pocket is stabilized through the attractive non-covalent T-shaped  $\pi$ - $\pi$  interaction,  $\pi$ -cation interactions and  $\pi$ -alkyl interactions between the aromatic rings of THP with the amino acid residues suggest that through these interactions the ligand THP binds with albumin protein that inhibits the synthesis of phosphodiesterase enzyme and other mediators in the process of improving its anti-asthmatic activity.

### Acknowledgements

The author Y.Sheeba Sherlin thanks the University Grants Commission (UGC), India for conferring a Teacher Fellowship under Faculty Development Programme leading to Ph.D. The author T.Vijayakumar acknowledges the Department of Space, Government of India for RESPOND project and SRM University, Chennai for selective excellence initiative.

### References

1. H.Smith, A review of bronchodilators for chronic obstructive pulmonary disease, *S Afr Pharm J*,80 (2013) 9-12.
2. K.M.Piafsky, R.I.Ogilvie, Dosage of theophylline in bronchial asthma, *The new England journal of medicine*, 292 (1975) 1219-22.
3. J.W.Jenne, Theophylline as a Bronchodilator in COPD and Its Combination with Inhaled  $\beta$  Adrenergic Drugs.
4. S.Gunasekaran, G.Sankari, S.Ponnusamy, Vibrational spectral investigation on xanthine and its derivatives-theophylline, caffeine and theobromine, *Spectrochimica Acta Part A* 61 (2005) 117–127.
5. J. P. Monteiro, M.G. Alves, P.F. Oliveira and B.M. Silva, Structure-Bioactivity Relationships of Methylxanthines: Trying to Make Sense of All the Promises and the Drawbacks, *molecules*, 21 (2016) 1-32.
6. A.A.Bunaciu, H.Y.A.Enein, Vibrational Spectroscopy Applications in Drugs Analysis, *Encyclopedia of Spectroscopy and Spectrometry*, Third Edition, 4 (2017) 575-581.
7. L.M.Moreira, L.Silveira, F.V.Santos, J. P. Lyon, R.Rocha, R.A. Zângaro, A. B.Villaverde and M.T.T. Pacheco, Raman spectroscopy: A powerful technique for biochemical analysis and diagnosis, *Spectroscopy* 22 (2008) 1-9.
8. S.Wartewiga, R.H.H. Neubertb, Pharmaceutical applications of Mid-IR and Raman spectroscopy, *Advanced Drug Delivery Reviews*, 57 (2005) 1144– 1170.
9. M. J. Frisch, G. W. Trucks, H. B. Schlegel, G. E. Scuseria, M. A. Robb, J. R. Cheeseman, G. Scalmani, V. Barone, G. A. Petersson, H. Nakatsuji, X. Li, M. Caricato, A. Marenich, J. Bloino, B. G. Janesko, R. Gomperts, B. Mennucci, H. P. Hratchian, J. V. Ortiz, A. F. Izmaylov, J. L. Sonnenberg, D. Williams-Young, F. Ding, F. Lipparini, F. Egidi, J. Goings, B. Peng, A. Petrone, T. Henderson, D. Ranasinghe, V. G. Zakrzewski, J. Gao, N. Rega, G. Zheng, W. Liang, M. Hada, M. Ehara, K. Toyota, R. Fukuda, J. Hasegawa, M. Ishida, T. Nakajima, Y. Honda, O. Kitao, H. Nakai, T. Vreven, K. Throssell, J. A. Montgomery, Jr., J. E. Peralta, F. Ogliaro, M. Bearpark, J. J. Heyd, E. Brothers, K. N. Kudin, V. N. Staroverov, T. Keith, R. Kobayashi, J. Normand, K. Raghavachari, A. Rendell, J. C. Burant, S. S. Iyengar, J. Tomasi, M. Cossi, J. M. Millam, M. Klene, C. Adamo, R. Cammi, J. W. Ochterski, R. L. Martin, K. Morokuma, O. Farkas, J. B. Foresman, and D. J. Fox, *Gaussian 09*, Revision A.02, Gaussian, Inc., Wallingford CT, 2009.
10. M. P.Andersson, P. Uvdal , New Scale Factors for Harmonic Vibrational Frequencies Using the B3LYP Density Functional Method with the Triple - $\zeta$  Basis Set 6-311+G(d,p *J. Phys. Chem.A*, 109 (12), (2005), 2937–2941.
11. M.H. Jamróz, *Vibrational Energy Distribution Analysis: VEDA 4*, program, Warsaw, 2004-2010. <http://www.smmg.pl/software/veda>.

12. M.H. Jamróz, "Vibrational Energy Distribution Analysis (VEDA): Scopes and limitations", *Spectrochimica Acta Part A: Molecular and Biomolecular Spectroscopy*, 114 (2013) 220-230.
13. D.Khamar ,R.G.Pritchard, I.J.Bradshaw, G.A.Hutcheon and L.Seton, Polymorphs of anhydrous theophylline: stable form IV consists of dimer pairs and metastable form I consists of hydrogen-bonded chains *Acta Crystallographica C* 67 (2011) 0496-0499.
14. Daimay Lin-Vien, Norman B .Colthup, William G .Fateley, Jeanette G .Grasselli, *The Handbook of Infrared and Raman Characteristic Frequency of Organic molecules*, Academic Press, New York (1991).
15. G.Socrates, *Infrared characteristic group frequencies* , John wiley & sons, New York (1980).
16. C.James, C.Ravikumar, V.S.Jayakumar, I. Hubert Joe, *Raman spectroscopy*, 40 (2009), 537-545.
17. H.G.M. Edwards, T. Munshi, M. Anstis, Raman spectroscopic characterisations and analytical discrimination between caffeine and demethylated analogues of pharmaceutical relevance, *Spectrochimica Acta Part A* 61 (2005) 1453–1459.
18. S.Stanchev, J.Mitkov,M.Georgieva,and A.Zlatkov, DFT Study of the Physicochemical characteristics and Spectral Behavior of New 8-Substituted 1,3,7-Trimethylxanthines, *International Journal of Quantum Chemistry*,112 (2012) 1-10.
19. T.Vijayakumar, I.Hubert Joe, C.P.Reghunadhan Nair,V.S.Jaya Kumar, *Journal of Molecular Structure*, 877, (2008), 20-35.
20. T.Vijayakumar, I.Hubert Joe, C.P.Reghunadhan Nair and V.S.Jayakumar, Vibrational spectral studies on charge transfer and ionic hydrogen-bonding interactions of nonlinear optical material L-arginine nitrate hemihydrate *J. Raman Spectrosc.* 40 (2009) 18-30.
21. T.Vijayakumar, I.Hubert Joe, C.P.Reghunadhan Nair and V.S.Jayakumar, Efficient  $\pi$ - electrons delocalization in prospective push–pull non-linear optical chromophore 4-[N,N-dimethylamino]-4-nitro stilbene (DANS): A vibrational spectroscopic study *Chemical Physics* 343 (2008) 83-99.
22. P.J.Barnes, *Theophylline, Pharmaceuticals*, 3 (2010) 725–747.
23. Y.S.Sherlin, T. Vijayakumar, J. Binoy, S.D.D. Roy, V.S. Jayakumar, Büchi's model based analysis of local anesthetic action in procaine hydrochloride: Vibrational spectroscopic approach, *Spectrochimica Acta Part A: Molecular and Biomolecular Spectroscopy* 205 (2018) 55–65.
24. S. Dobrinas, A. Soceanu, V. Popescu, G. Stanciu, S. Smalberger, Optimization of a UV-Vis spectrometric method for caffeine analysis in tea, coffee and other beverages,*Scientific Study & Research*, 14 (2013) 071 – 078.
25. P.A Zunszain, J.Ghuman, A.F.McDonagh, S.Curry, Crystallographic analysis of human serum albumin complexed with 4Z, 15E-bilirubin-IXalpha, *J. Mol. Biol.* 381 (2008) 394-406.